SUPPLEMENTARY MATARIAL

Supplement to: Knabl L., Mitra T., Kimpel J. et al.,

High SARS-CoV-2 Seroprevalence in Children and Adults in the Austrian Ski Resort Ischgl

TABLE OF CONTENT

List of investigators	3
List of voluntary members of the study team	4
Supplementary methods	5
SUPPLEMENTARY FIGURES	7
Figure S1. Study enrollment	7
Figure S2. Correlation of anti-S with anti-N antibodies	8
Figure S3. Neutralizing antibodies	9
Figure S4. Titers of neutralizing antibodies correlate with anti-S IgG titers	10
Figure S5. Age distribution of antibody and viral RNA detection	11
SUPPLEMENTARY TABLES	12
Table S1. Characterizing study participants with current PCR-confirmed SARS-CoV-2 infection	12
Table S2 Household level analysis of sero status by number of children in household	13
SUPPLEMENT: MATHEMATICAL MODEL	14

LIST OF INVESTIGATORS

Investigator	Affiliation
Ludwig Knabl	Institute of Virology, Department of Hygiene, Microbiology and Public Health, Medical University of Innsbruck, Austria
Tanmay Mitra	Department of Systems Immunology and Braunschweig Integrated Centre of Systems Biology, Helmholtz Centre for Infection Research, Braunschweig, Germany
Janine Kimpel	Institute of Virology, Department of Hygiene, Microbiology and Public Health, Medical University of Innsbruck, Austria
Annika Rössler	Institute of Virology, Department of Hygiene, Microbiology and Public Health, Medical University of Innsbruck, Austria
André Volland	Institute of Virology, Department of Hygiene, Microbiology and Public Health, Medical University of Innsbruck, Austria
Andreas Walser	Dr. Walser's surgery, Ischgl, Austria
Hanno Ulmer	Department of Medical Statistics, Informatics and Health Economics, Medical University of Innsbruck, Austria
Lisa Pipperger	Institute of Virology, Department of Hygiene, Microbiology and Public Health, Medical University of Innsbruck, Austria
Sebastian C. Binder	Department of Systems Immunology and Braunschweig Integrated Centre of Systems Biology, Helmholtz Centre for Infection Research, Braunschweig, Germany
Lydia Riepler	Institute of Virology, Department of Hygiene, Microbiology and Public Health, Medical University of Innsbruck, Austria
Katie Bates	Department of Medical Statistics, Informatics and Health Economics, Medical University of Innsbruck, Austria
Arnab Bandyopadhyay	Department of Systems Immunology and Braunschweig Integrated Centre of Systems Biology, Helmholtz Centre for Infection Research, Braunschweig, Germany
Marta Schips	Department of Systems Immunology and Braunschweig Integrated Centre of Systems Biology, Helmholtz Centre for Infection Research, Braunschweig, Germany
Mrinalini Ranjan	Department of Systems Immunology and Braunschweig Integrated Centre of Systems Biology, Helmholtz Centre for Infection Research, Braunschweig, Germany
Barbara Falkensammer	Institute of Virology, Department of Hygiene, Microbiology and Public Health, Medical University of Innsbruck, Austria
Wegene Borena	Institute of Virology, Department of Hygiene, Microbiology and Public Health, Medical University of Innsbruck, Austria
Michael Meyer-Hermann	Department of Systems Immunology and Braunschweig Integrated Centre of Systems Biology, Helmholtz Centre for Infection Research, Braunschweig, Germany
Dorothee von Laer	Institute of Virology, Department of Hygiene, Microbiology and Public Health, Medical University of Innsbruck, Austria

LIST OF VOLUNTARY STUDY MEMBERS, ALL FROM AUSTRIA

Sebastian Eiter	Stefan Mayer
Albert Falch	Eva Meindl
Maximillian Freilinger	Bianca Neurauter
Peter Fröhlich	Cornelia Ower
Carina Gatt	David Pap
Teresa Grässl	Daniel Pichler
Rosmarie Gstraunthaler	Manfred Primisser
Teresa Harthaller	Juliana Reisenzahn
Emmanuel Heilmann	Bernadette Röttig
Luzia Hoch	Magdalena Sacher
Jonas Huber	Nadine Schedler
Maria Huber	Valentin Schiessendoppler
Benedikt Hutzler	Peter Slamnig
Cornelia Kindl	Maximillian Tschallener
Martin Klieber	Katrin Wabro
Michelle Liu	Paula Wunsch

SUPPLEMENTARY METHODS

Viral RNA detection from throat swabs

Viral RNA was extracted from the virus transport media (CDC, SOP#: DSR-052-01) using the EasyMag® NucliSENS® System (bioMérieux, Marcy-l'Étoile, France). RT-PCR for the detection of SARS-CoV-2 was performed using the RealStar® SARS-CoV-2 RT-PCR kit 1.0 (Altona Diagnostics GmbH, Hamburg, Germany) on the CFX96TM Real-Time System (Bio-Rad, Feldkirchen, Germany) according to the manufacturers' instructions. Ct values below 40 in the PCR were rated as positive and confirmed by a second PCR. The district administration provided results of previous SARS-CoV-2 PCR tests in Ischgl, which had been performed between March 1 and April 20, 2020.

Viral antibody testing

Participants' sera were screened for anti-SARS-CoV-2-S1-protein IgA and IgG positivity by a commercially available anti-SARS-CoV-2-IgA and -IgG ELISA (Euroimmun, Lübeck, Germany), respectively, using the fully automated 4-plate benchtop instrument Immunomat™ (Virion/Serion, Würzburg, Germany). Results with respect to the obtained optical density (OD) values were interpreted according to the recommendations in the manufacturer's information. Samples with a borderline (O.8-1.1) result were repeatedly tested and considered positive in case of another borderline result. Additionally, each serum was tested for anti-SARS-CoV-2-N-protein IgG (anti-N IgG) with the Abbott SARS-CoV-2 IgG immunoassay on the ARCHITECT i2000SR system (Abbott, Illinois, USA). Anti-N IgG was positive, if the obtained relative light unit (RLU) value corresponded to the manufacturer's recommendations (>1.4).

For the neutralizing antibody assay, Vero cells expressing TMPRSS2 were kindly provided by Dr. Markus Hoffmann and Prof. Stefan Pöhlmann [5]. SARS-CoV-2 was isolated from a patients' respiratory swab sample in Innsbruck (isolate 1.2) and virus stocks were produced on Vero/TMPRSS2 cells. Participants' plasma was heat inactivated at 56°C for 30 min. Subsequently, it was centrifuged for 5 minutes at 8,000 rpm in a tabletop centrifuge. 4-fold plasma dilutions were mixed with an equal volume of SARS-CoV-2 virus (1.2 isolate) resulting in ~300 infected cells in non-neutralized wells. Plasma/virus mixes were incubated for 1 hour at 37°C and subsequently transferred to 96-wells containing 90% confluent Vero/TMPRSS2 seeded one day before. Cells were infected with the virus for 1 hour at 37°C and subsequently washed once, fresh complete medium containing 2% FCS was added and cells were further cultured for 13 hours. Cells were fixed for 5 minutes with 96% ethanol and subsequently stained using the serum from a SARS-CoV-2 recovered patient and a horse radish peroxidase (HRPO)-conjugated anti-human secondary antibody (Dianova, Hamburg, Germany). Plates were developed using 3-amino-9-ethylcarbazole (AEC) substrate. Infected cells were counted in the microscope and 50% neutralization titers were calculated as highest dilution where mean infection of duplicate samples was lower than 50% of the mean of control wells without serum.

Household analysis

Sero-status of households with no, 1 or more than 2 children was analyzed. Individuals with unknown household affiliation (n=106) were excluded from the analysis. Household sero status was defined as "positive" (all members positive), "negative" (all members negative) and "mixed" (members both positive and negative). Descriptive statistics were used to describe the household sero status for the whole population, as well as among households with children. An individual level logistic regression model was run for sero status by children/adults for all participants in households with children.

SUPPLEMENTARY FIGURES

(Material and Methods as in main manuscript)

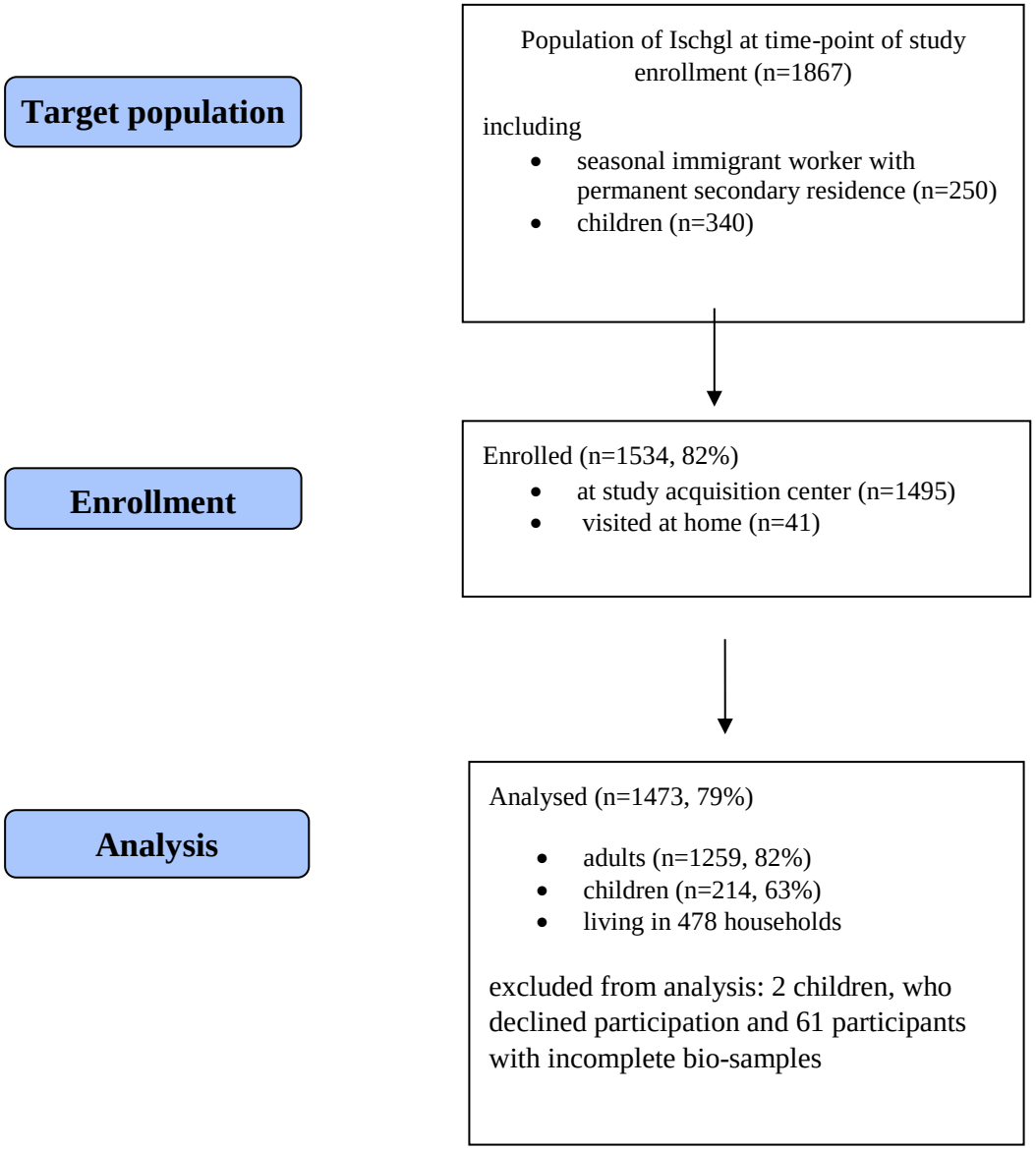

Figure S1. Study enrollment. The target population for this cross-sectional study consisted of the Ischgl population at the time-point of the survey (n=1867 inhabitants with main residence in Ischgl including 250 seasonal immigrant workers with permanent secondary residence). While 1495 study participants appeared at the study acquisition center, 41 were visited at home by the general practitioner. Due to incomplete bio-samples from 61 individuals and 2 exclusions in the pediatric cohort due to decline of participation, a total of 1473 study participants from 478 households were included into statistical analysis. As the study was anonymous and some individuals did not visit the study center together with the rest of the household members, 106 individuals could not be assigned to a household. Overall participation rate for analysis was 79%.

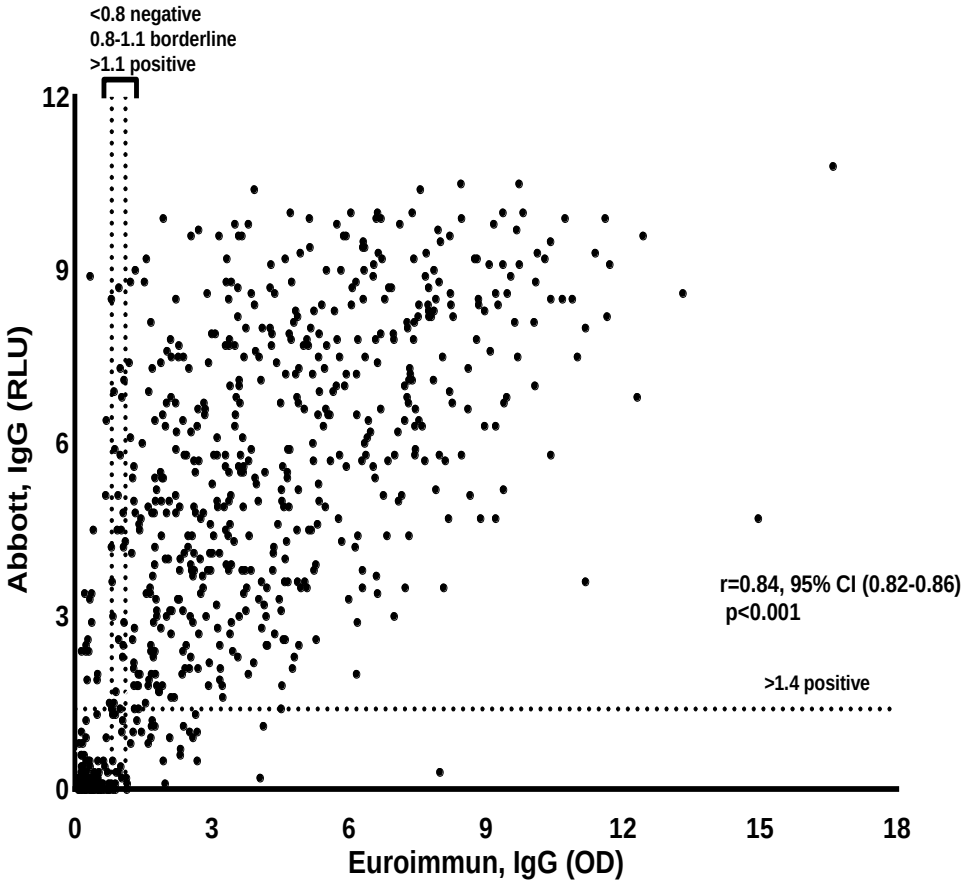

Figure S2. Correlation of anti-S with anti-N IgG antibodies to SARS-CoV-2. Anti-S-IgG (Euroimmun) plotted against anti-N-IgG (Abbott) in plasma samples of 1473 study participants with Spearmans correlation coefficient (r) and 95% confidence interval (CI) of the coefficient. Dotted horizontal line represents the cutoff value for Abbott IgG test. Dotted vertical lines indicate negative (<0.8), borderline (0.8-1.1) and positive (>1.1) cutoff values for Euroimmun anti-S-IgG test.
RLU= relative light unit, OD=Optical density

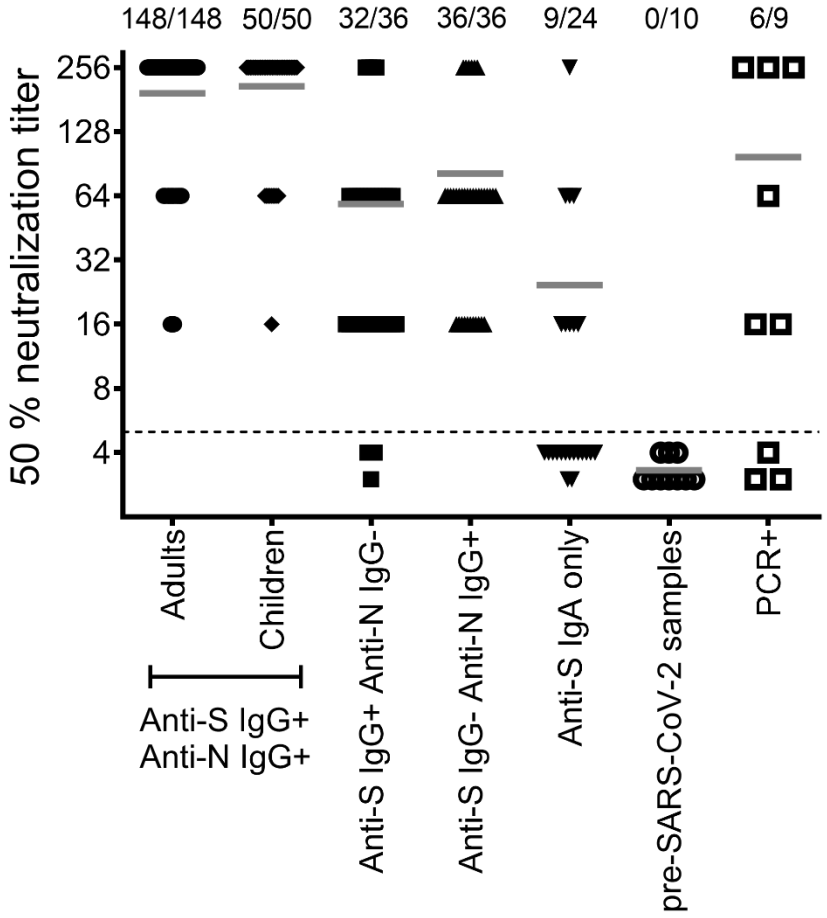

Figure S3. Neutralizing antibody titers in seropositive individuals. 50% neutralization titers were determined using a replication competent SARS-CoV-2 isolate. Numbers above the graph indicate number positive samples/total number tested (n=148 for anti-S IgG+/anti-N IgG+ adults, n=50 for anti-S IgG+/anti-N IgG+ children, n=36 for anti-S IgG+/anti-N IgG-, n=36 for anti-S IgG-/anti-N IgG+, n=24 for only anti-S IgA+, n=10 for plasma samples obtained before the SARS-CoV-2 pandemic, and n=9 for PCR positive individuals found in the study. Among the PCR positive samples were 3 anti-S IgG+/anti-N IgG+, 1 anti-S IgG+/anti-N IgG-, 2 only anti-S IgA+, and 3 anti-S IgG-/anti-N IgG-. Shown are mean and individual samples. Dashed line shows cut-off for the neutralization assay (>1:4).

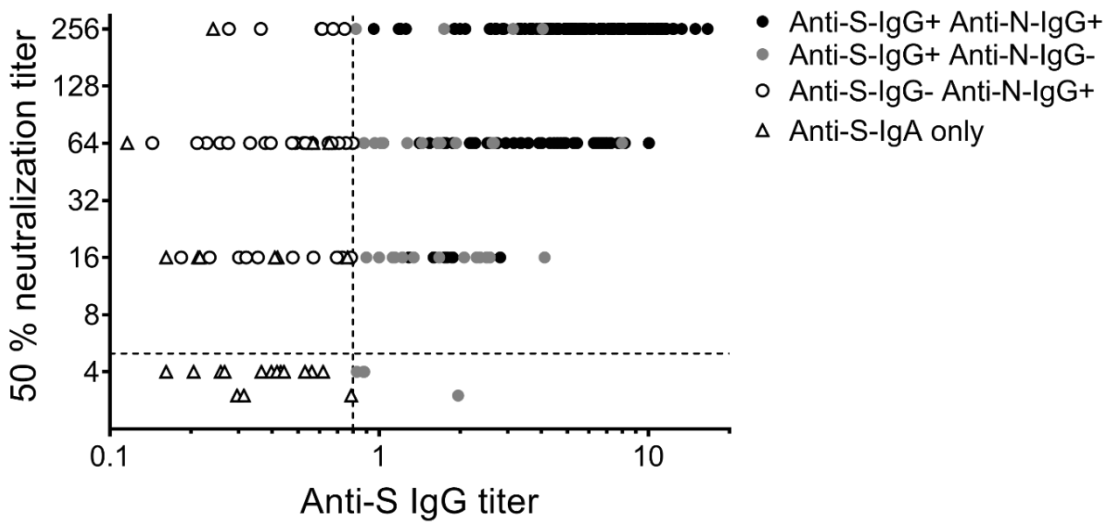

Figure S4. Titers of neutralizing antibodies correlate with anti-S IgG levels. Plasma samples were analyzed via ELISA for titers of Anti-S IgG antibodies and via neutralization assay using replication competent SARS-CoV-2 for 50% neutralization titers. Each data point represents an individual plasma sample; n=201 for anti-S IgG+/anti-N IgG+ (50 children and 151 adults); n= 37 for anti-S IgG+/anti-N IgG-; n=36 for anti-S IgG-/anti-N IgG+; n=26 for solely anti-S IgA positive subjects. Dashed lines show cut-off for neutralization assay (>1:4) and anti-S IgG ELISA (≥0.8).

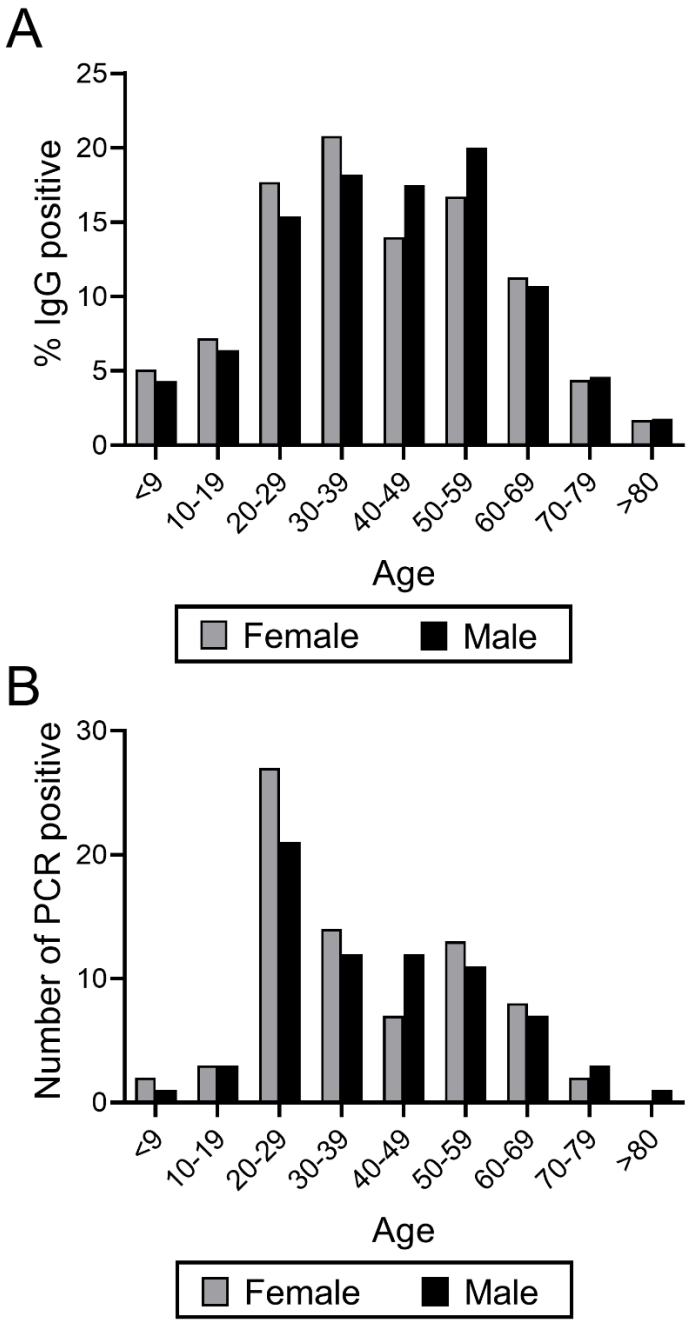

Figure S5. Children likely underdiagnosed by SARS-CoV-2 PCRs performed in Ischgl to a greater extent than adults.

A. Age distribution of seroprevalence among study participants in Ischgl. y-axis: percent antibody positive of total population, x-axis: age in years. B. Age-distribution of positive SARS-CoV-2 PCR tests among age- and sex- groups in Ischgl. Data were kindly provided by the Austrian Agency for Health and Food Safety (AGES GmbH). y-axis: percent positive of all SARS-CoV-2 PCR tests performed in Austria, x-axis: age in years.

SUPPLEMENTARY TABLES

Table S1. Characterizing study participants with current PCR-confirmed SARS-CoV-2 infection (n=9)

Participant ID	Age	Sex	PCR CT	Antibody				Previous symptoms	Time since symptom onset	Current symptoms
				Anti S IgA (ODratio*)	Anti S IgG (ODratio)*	Anti N IgG (RLU)**	Neutralization assay [§]			
9284198	23	female	38.1	0.5	0.22	0.1	<1:4	None	-	None
9283484	44	male	38.9	4.21	0.79	0.1	<1:4	None	-	None
9174286	55	female	36.1	1.29	5.72	7	1:256	Anosmia, GI symptoms	39 days	None
9313178	59	male	37.2	2.37	7.44	6.3	1:256	None	-	None
9267090	16	male	38.2	0.11	0.11	0	1:16	None	-	None
9267864	6	female	35.2	1.33	0.41	0	1:16	None	-	None
9249920	13	male	38.2	0.62	0.29	0	1:4	GI symptoms	37 days	None
9176591[#]	78	male	33.3	4.73	8	9.5	1:256	Cough, fever, breathing difficulties, sore throat, anosmia, dysgeusia, GI symptoms	25 days	None
9313477	27	male	30.3	0.72	0.96	0.3	1:64	Anosmia, dysgeusia	35 days	None

# PCR positivity known (32days before study begin); * ODratio <0.8 =negative. 0.8 - 1.1=borderline. >1.1= positive ; ** RLU>1.40 positive; [§]cutoff: >1:4=positive, ≤1:4=negative
CT=cycle threshold. OD= optical density. RLU= relative light unit. S= spike protein. N= nucleocapsid protein

Table S2 Household level analysis of sero status by number of children in household

Sero status of Household	Number of Households	% within Household Type	% of All Household
Household with no children			
Mixed	108	30.5	22.6
Negative	150	42.4	31.4
Positive	96	27.1	20.1
Household with one child			
Mixed	30	60	6.3
Negative	15	30	3.1
Positive	5	10	1.0
Household with 2+ children			
Mixed	49	66.2	10.3
Negative	19	25.7	4.0
Positive	6	8.1	1.3
Total	478		100

Supplementary Information for Mathematical Model

Supplementary Figures:

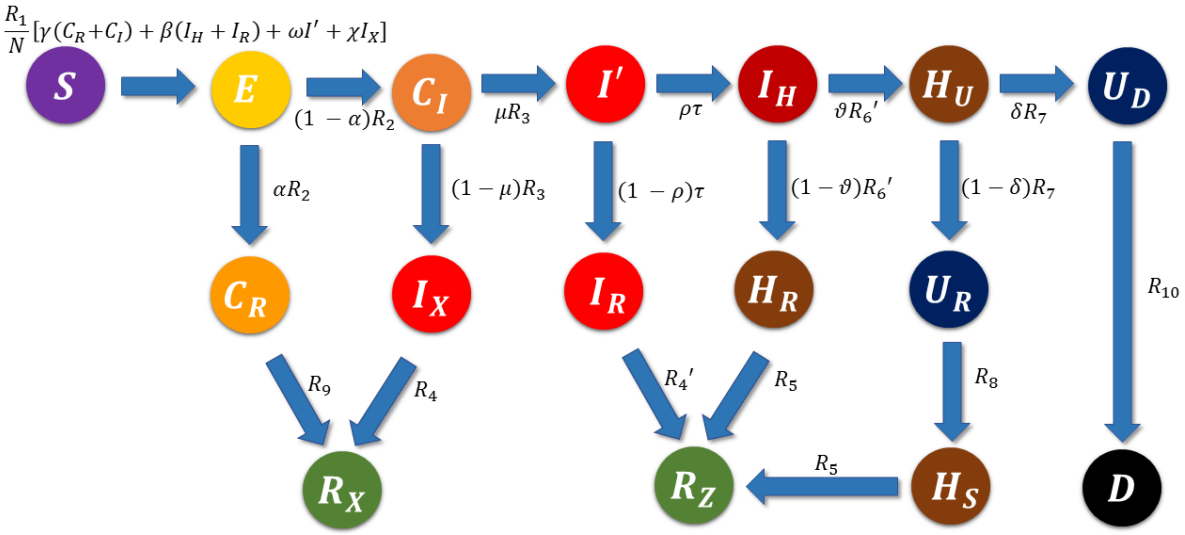

Figure MS1. Model used to study COVID-19 outbreak in Ischgl. A compartment model inspired by [1] was calibrated to simulate the dynamics of the outbreak in Ischgl. For information regarding specific compartments, see Figure MS2.

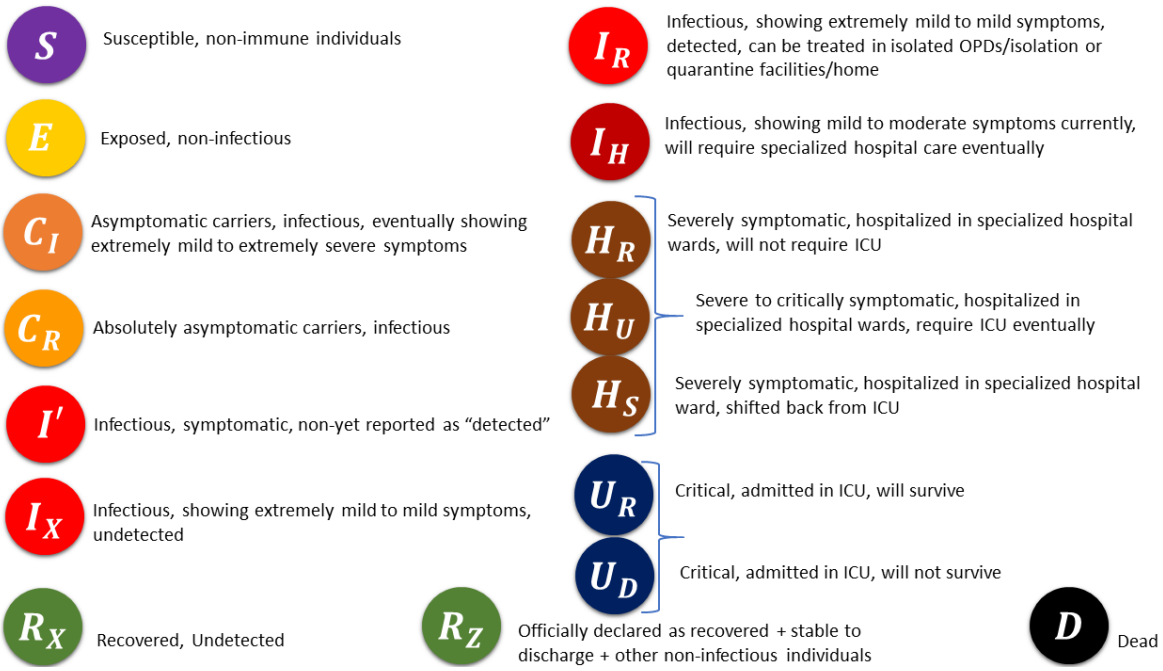

Figure MS2. Specific description of the compartments of the model in Figure MS1.

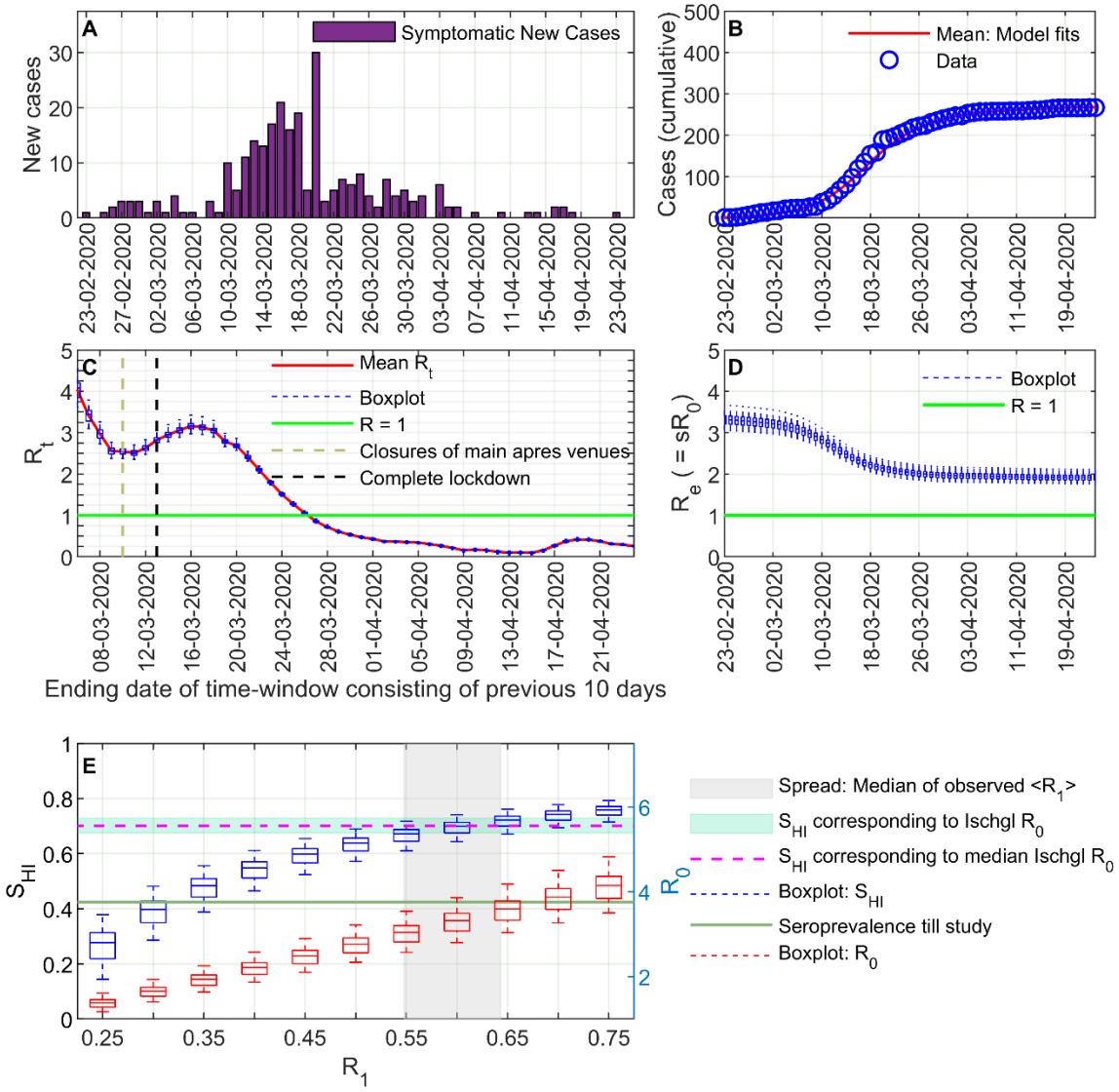

Figure MS3. Analysis based on epidemic curve constructed with temporal data for onset of anosmia/dysgeusia among the seropositive individuals. The time-course of new COVID-19 cases in Ischgl based on anosmia/dysgeusia among seropositive individuals as obtained from the survey **(A)** was used to determine the model parameters (see fitting strategy in supplementary information). The calibrated model reproduces the cumulative number of anosmia/dysgeusia cases **(B)** and predicts the time-dependent reproduction number R_t **(C)**. Time-dependent alterations in the effective reproduction number R_e **(D)** measured in terms of $R_e = sR_0$, s being the fraction of the susceptible population at a certain time. **(E)** Seroprevalence necessary for herd immunity (S_{HI}, green shaded region) and basic reproduction number (R_0, red box plots) are shown as functions of the contact dependent transmission rate (R_1). The analysis was done with the parameter sets (except R_1) best describing the case numbers until Mar 16 at a full stretch (see fitting strategy in the supplementary information). R_0 in Ischgl was between 3.1 to 3.7, with a median value of 3.3, which corresponds to a median value of 69.7% seroprevalence to reach herd immunity (S_{HI} corresponding to median R_0, purple line). This is consistent with herd-immunity seroprevalence (blue box plot) derived from the median contact dependent daily transmission rate $< R_1 >$ for the time-windows spanning Feb 23 – Mar 16 and Feb 28 – Mar 16 (grey patch). The achieved seroprevalence (green line) is substantially lower than the thresholds. Note that we considered the survey-oriented symptomatic cases before Feb 23, 2020 as asymptomatic cases of COVID-19 due to having comparably lower odds ratio (OR) than that of March 2020 and suspected overlap with the flu-season in Ischgl. In addition, for this analysis, cases that did not report onset of anosmia/dysgeusia from Feb 23, 2020 were also considered to be asymptomatic due to significantly higher OR for anosmia/dysgeusia as compared to any other symptom.

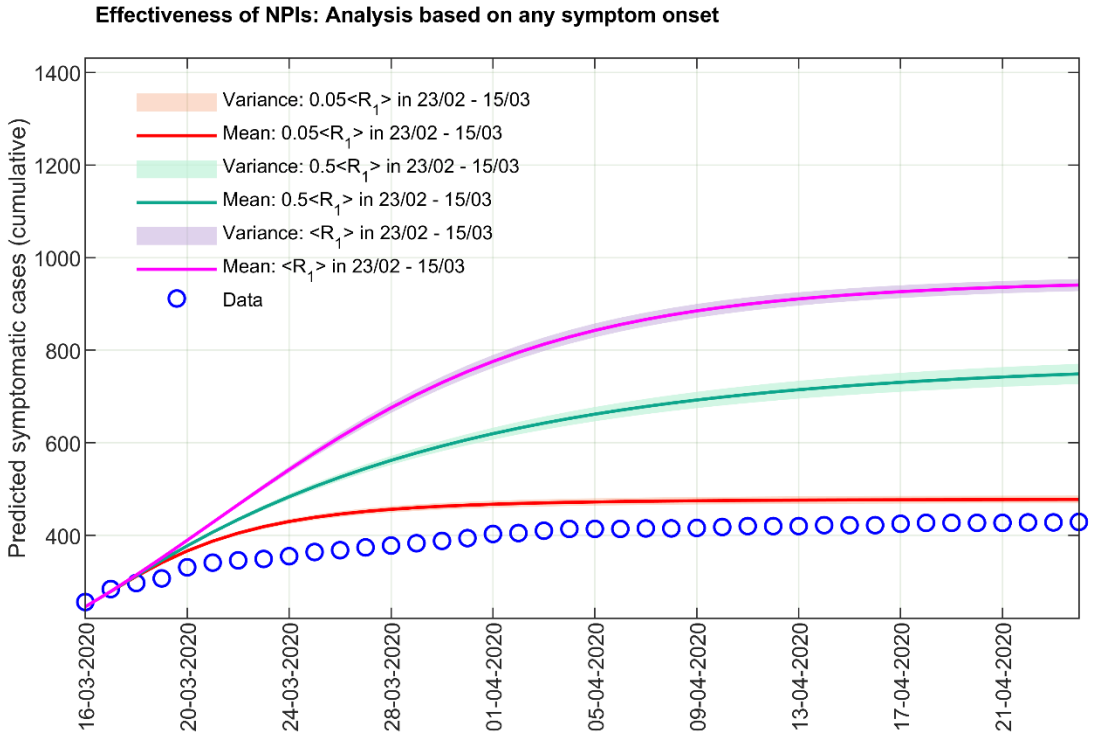

Figure MS4. Mathematical modelling suggests the effectiveness of the implemented NPIs in Ischgl. Different scenarios for the future time-course of the outbreak after mid-March were projected until April 24, 2020 using three different contact dependent transmission rates (R_1), viz., 100% (pink), 50% (green) and 5% (red) of the observed $< R_1 >$ during the time spanning Feb 23 to Mar 15, 2020, along with the survey-oriented Ischgl case data (blue dots) during the same period. The lines depict the average time course and the shaded areas show the variance of the simulated results. A substantial difference between the observed data and simulated results with unrestricted transmission rate of $< R_1 >$ during Feb 23 to Mar 15, 2020 suggested the effectiveness of NPIs in Ischgl. Note that we considered the survey-oriented symptomatic cases before Feb 23, 2020 as asymptomatic cases of COVID-19 due to having comparably lower odds ratio (OR) than that of March 2020 and suspected overlap with the flu-season in Ischgl.

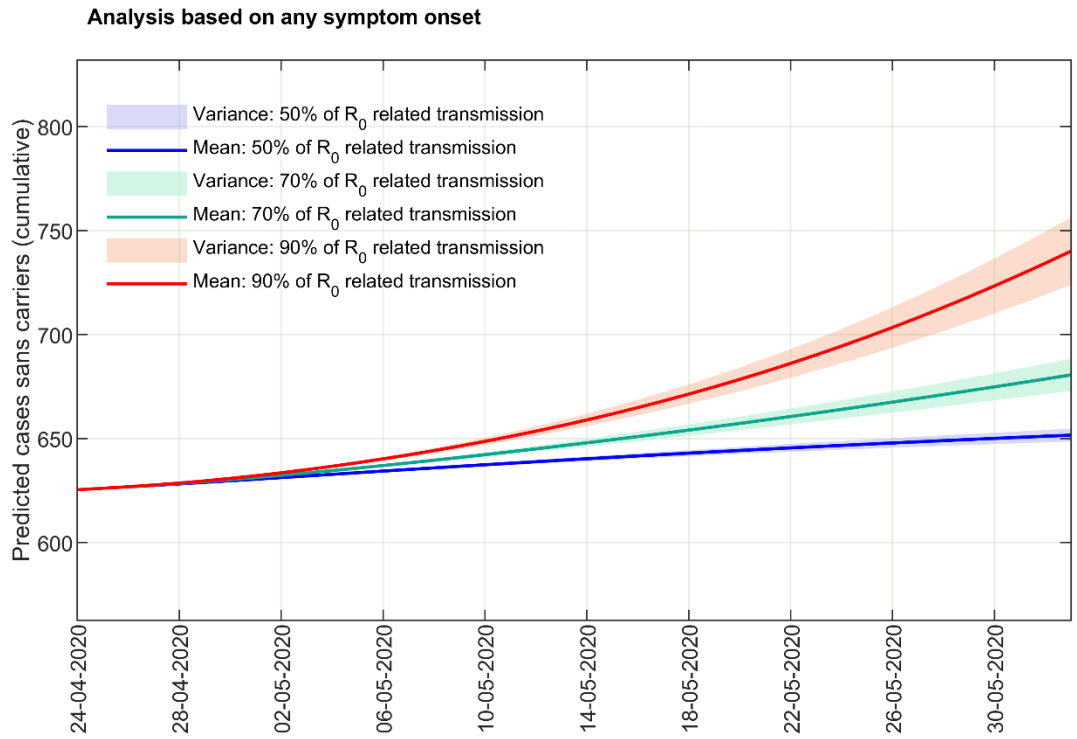

Figure MS5. Without NPIs, if the ski resort continued its activity as the way it was doing before closures, the village could face a new outbreak even after April 2020. Different scenarios for the future time-course of the outbreak after April 24, 2020 were projected until start of June 2020 using three different reproduction numbers, viz., 90% (red), 70% (green) and 50% (blue) of the observed basic reproduction number, R_0 as obtained from fitting the Ischgl case data till Mar 16 when the virus was spreading without the effect of the restrictions in place (see fitting strategy in the supplementary information). The lines depict the average time course and the shaded areas show the variance of the simulated results. A substantial increase in the predicted number of cases in case of viral spreading with a value close to R_0 suggested that the ski resort could face a new outbreak without the NPIs in place. This also supported that the village was still away from achieving herd immunity. Note that we considered the survey-oriented symptomatic cases before Feb 23, 2020 as asymptomatic cases of COVID-19 due to having comparably lower odds ratio (OR) than that of March 2020 and suspected overlap with the flu-season in Ischgl.

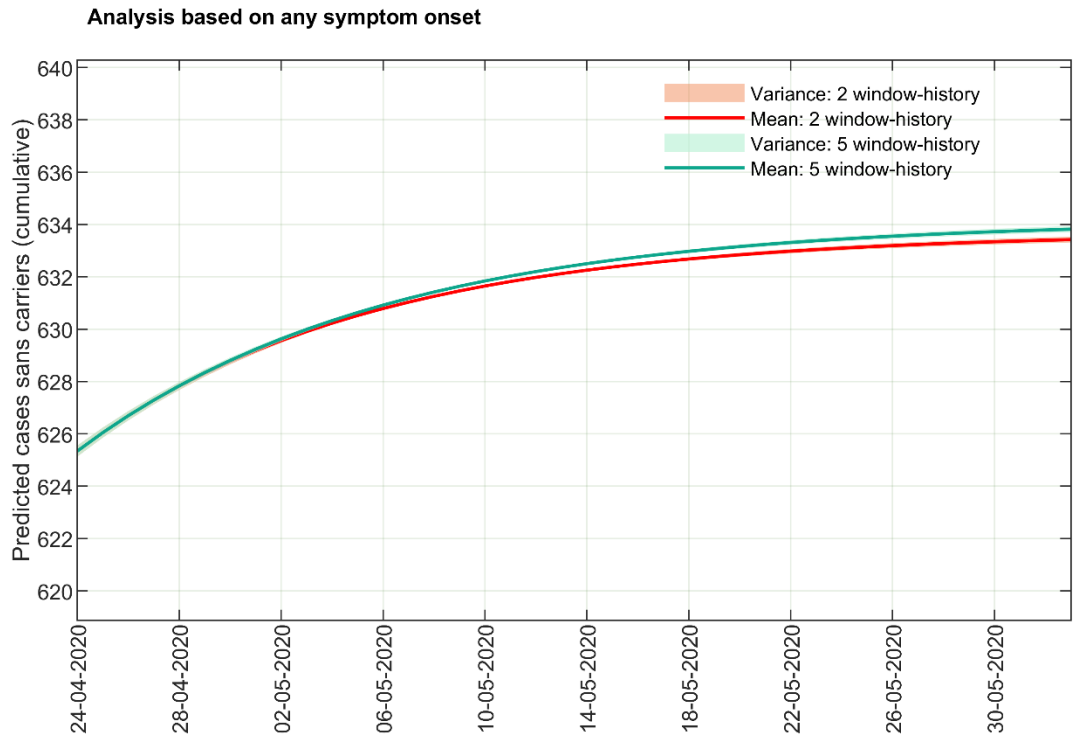

Figure MS6. Keeping the transmission rate as it is in the ski resort after April 2020 would ensure no significant increase in new infections. Different scenarios for the future time-course of the outbreak after April 24, 2020 were projected until start of June 2020 using the history of contact dependent transmission rates (R_1) in two recent past time-windows, viz., $< R_1 >$ in the last 5 (green) and the last 2 (red) time-windows ending on April 24 2020. The lines depict the average time course and the shaded areas show the variance of the simulated results. Both scenarios did not result in a substantial increase in the predicted number of cases in the ski resort. Note that we considered the survey-oriented symptomatic cases before Feb 23, 2020 as asymptomatic cases of COVID-19 due to having comparably lower odds ratio (OR) than that of March 2020 and suspected overlap with the flu-season in Ischgl.

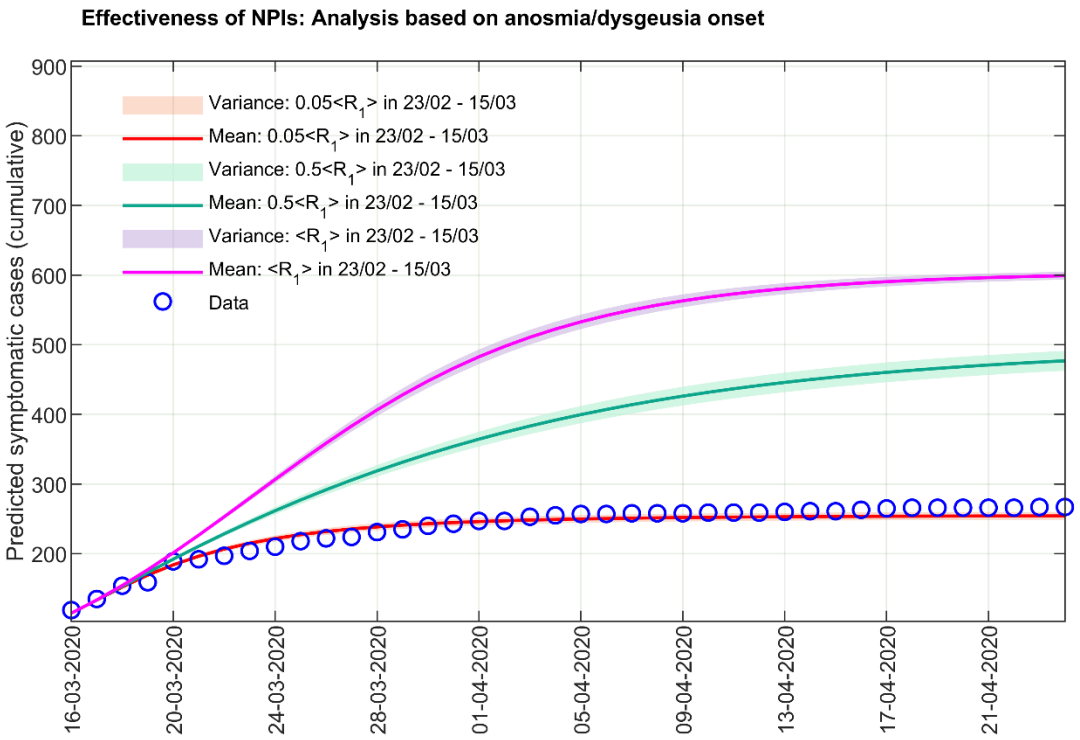

Figure MS7. Mathematical modelling suggests the effectiveness of the implemented NPIs in Ischgl using anosmia/dysgeusia data. Different scenarios for the future time-course of the outbreak after mid-March were projected until April 24, 2020 using three different contact dependent transmission rates (R_1), viz., 100% (pink), 50% (green) and 5% (red) of the observed $< R_1 >$ during the time spanning Feb 23 to Mar 15, 2020, along with the survey-oriented Ischgl anosmia/dysgeusia case data (blue dots) during the same period. The lines depict the average time course and the shaded areas show the variance of the simulated results. A substantial difference between the observed anosmia/dysgeusia data and simulated results with unrestricted transmission rate of $< R_1 >$ during Feb 23 to Mar 15, 2020 suggested the effectiveness of NPIs in Ischgl. Note that we considered the survey-oriented symptomatic cases before Feb 23, 2020 as asymptomatic cases of COVID-19 due to having comparably lower odds ratio (OR) than that of March 2020 and suspected overlap with the flu-season in Ischgl. In addition, for this analysis, cases that did not report onset of anosmia/dysgeusia from Feb 23, 2020 were also considered to be asymptomatic due to significantly higher OR for anosmia/dysgeusia as compared to any other symptom.

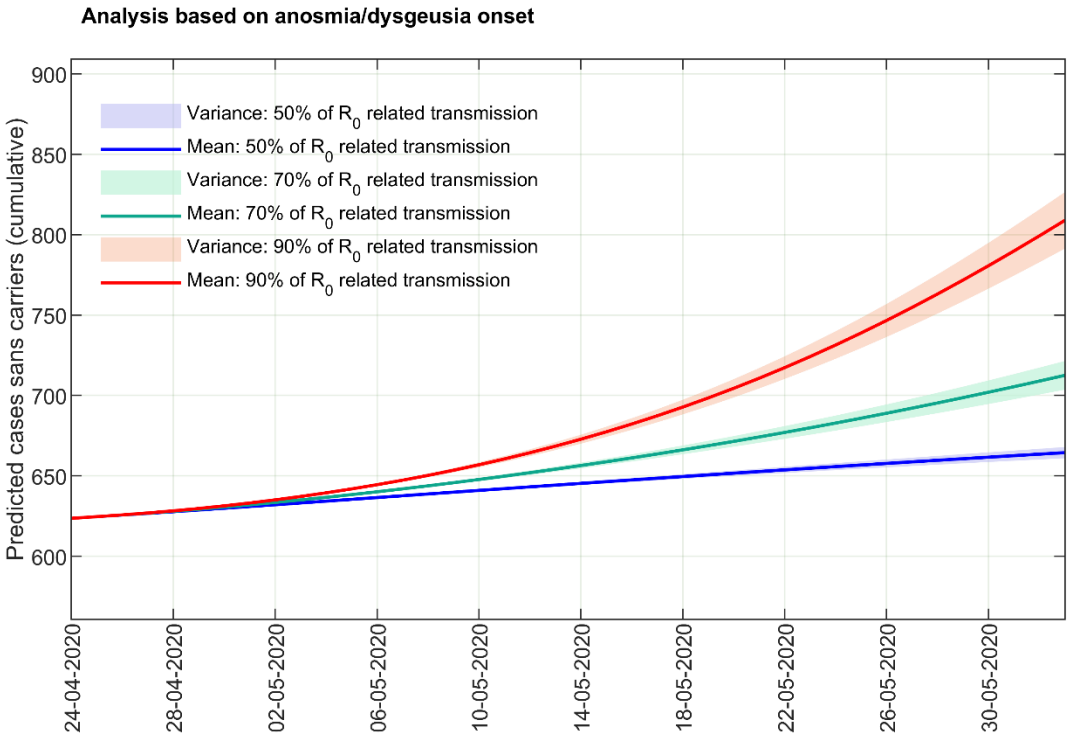

Figure MS8. Without NPIs, if the ski resort continued its activity as the way it was doing before closures, the village could face a new outbreak even after April 2020. Different scenarios for the future time-course of the outbreak after April 24, 2020 were projected until start of June 2020 using three different reproduction numbers, viz., 90% (red), 70% (green) and 50% (blue) of the observed basic reproduction number, R_0 as obtained from fitting the Ischgl anosmia/dysgeusia case data till mid-March when the virus was spreading without restrictions. The lines depict the average time course and the shaded areas show the variance of the simulated results. A substantial increase in the predicted number of cases in case of viral spreading with a value close to R_0 suggested that the ski resort could face a new outbreak without the NPIs in place. This also supported that the village was still away from achieving herd immunity. Note that we considered the survey-oriented symptomatic cases before Feb 23, 2020 as asymptomatic cases of COVID-19 due to having comparably lower odds ratio (OR) than that of March 2020 and suspected overlap with the flu-season in Ischgl. In addition, for this analysis, cases that did not report onset of anosmia/dysgeusia from Feb 23, 2020 were also considered to be asymptomatic due to significantly higher OR for anosmia/dysgeusia as compared to any other symptom.

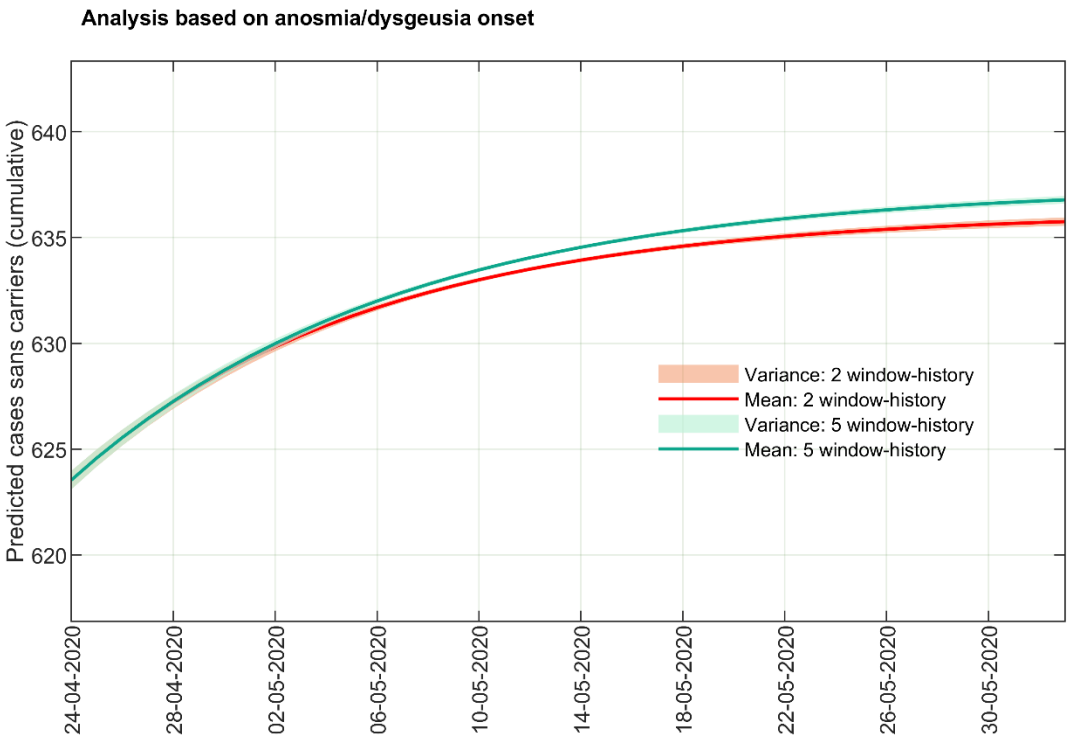

Figure MS9. Keeping the transmission rate as it is in the ski resort after April 2020 would ensure no significant increase in new infections. Different scenarios for the future time-course of the outbreak after April 24, 2020 were projected until start of June 2020 using the history of contact dependent transmission rates (R_1) in two recent past time-windows, viz., $< R_1 >$ in the last 5 (green) and the last 2 (red) time-windows ending on April 24 2020. The lines depict the average time course and the shaded areas show the variance of the simulated results. Both scenarios did not result in a substantial increase in the predicted number of cases in the ski resort. Note that we considered the survey-oriented symptomatic cases before Feb 23, 2020 as asymptomatic cases of COVID-19 due to having comparably lower odds ratio (OR) than that of March 2020 and suspected overlap with the flu-season in Ischgl. In addition, for this analysis, cases that did not report onset of anosmia/dysgeusia from Feb 23, 2020 were also considered to be asymptomatic due to significantly higher OR for anosmia/dysgeusia as compared to any other symptom.

Model equations [1]:

$$\frac{dS}{dt} = -\frac{R_1}{N}\left[\gamma(C_R + C_I) + \beta(I_H + I_R) + \omega I' + \chi I_X\right]S$$

$$\frac{dE}{dt} = \frac{R_1}{N}\left[\gamma(C_R + C_I) + \beta(I_H + I_R) + \omega I' + \chi I_X\right]S - R_2 E$$

$$\frac{dC_I}{dt} = (1-\alpha)R_2 E - R_3 C_I$$

$$\frac{dC_R}{dt} = \alpha R_2 E - R_9 C_R$$

$$\frac{dI'}{dt} = \mu R_3 C_I - \tau I'$$

$$\frac{dI_X}{dt} = (1 - \mu)R_3 C_I - R_4 I_X$$

$$\frac{dI_R}{dt} = (1-\rho)\tau I' - R_4{}' I_R$$

$$\frac{dI_H}{dt} = \rho\tau I' - R_6{}' I_H$$

$$\frac{dH_R}{dt} = (1-\vartheta)R_6{}' I_H - R_5 H_R$$

$$\frac{dH_U}{dt} = \vartheta R_6{}' I_H - R_7 H_U$$

$$\frac{dH_S}{dt} = R_8 U_R - R_5 H_S$$

$$\frac{dU_R}{dt} = (1-\delta)R_7 H_U - R_8 U_R$$

$$\frac{dU_D}{dt} = \delta R_7 H_U - R_{10} U_D$$

$$\frac{dR_X}{dt} = R_9 C_R + R_4 I_X$$

$$\frac{dR_Z}{dt} = R_4{}' I_R + R_5 H_R + R_5 H_S$$

$$\frac{dD}{dt} = R_{10} U_D$$

The set of coupled ordinary differential equations are integrated using the stiff solver ode15s implemented in *MATLAB Release 2018a*.

Model parameters:

Parameters with fixed value: $\gamma = 0.7,\ \omega = 1,\ \chi = 1,\ \mu = 1, \tau = 2, \vartheta = \frac{3}{11}, \delta = \frac{2}{3}$
For analysis with onset of any COVID-19 associated symptom since Feb 23, 2020, $\alpha = 0.3147, \rho = 0.026$
For analysis with onset of anosmia/dysgeusia since Feb 23, 2020, $\alpha = 0.5735, \rho = 0.0412$

Parameter	Estimated bounds	
	Min	Max
R_1	0.001	1.5
R_4	$\frac{1}{10}$	$\frac{1}{8}$
R_5	$\frac{1}{12}$	$\frac{1}{8}$
R_6	$\frac{1}{8}$	$\frac{1}{5}$
R_7	$\frac{1}{3}$	$\frac{1}{2}$
R_8	$\frac{1}{14}$	$\frac{1}{8}$
R_{10}	$\frac{1}{18}$	$\frac{1}{6.5}$
β	0.05	0.50

Table MS1. Estimated bounds used for data fitting to determine best parameter sets. See fitting strategy in the supplementary information. For details of estimation from literature, see [2].

Parameter constraints and relations:

1) $4.5 < \frac{1}{R_2} + \frac{1}{R_3} < 5.8$

   – considering 95% confidence interval of the incubation period [3]

2) $3.1 < \frac{1}{R_2} + \left(0.5 \times \frac{1}{R_3}\right) < 4.9$

   – considering 95% confidence interval of the serial interval [4]

3) $\frac{1}{R_2} > 1$

4) $\frac{1}{R_2} < \frac{1}{R_3}$

5) $\frac{1}{R_9} = \frac{1}{R_3} + (0.5 \times \frac{1}{R_4})$

6) $\frac{1}{R_4'} = \frac{1}{R_4} - \frac{1}{\tau}$

7) $\frac{1}{R_6'} = \frac{1}{R_6} - \frac{1}{\tau}$

Equation for R_0:

$$R_t = R_1(t)\frac{S(t)}{N(t)}\left[\frac{\gamma\alpha}{R_9} + \frac{\gamma(1-\alpha)}{R_3} + \frac{\chi(1-\alpha)(1-\mu)}{R_4} + \frac{\mu\omega(1-\alpha)}{\tau} + \frac{\beta\mu(1-\alpha)(1-\rho)}{R_4'} + \frac{\beta\mu\rho(1-\alpha)}{R_6'}\right]$$

We calculated R_0 using next generation method [5 – 7].

Data preparation for modelling:

In this study, the total number of serologically positive people who reported any symptom was: (624 - 136) + 2 = 490, 136 being the number of seropositive individuals who reported not to have any symptom and 2 being the number of total deaths (assumed to be seropositive before death). 29 seropositive persons had not given any symptom onset date and we did not know the symptom onset date of 2 dead persons. These two deaths in Ischgl occurred on 22nd of March and on 10th of April. From the bounds of the system parameters as mentioned in Table MS1, the time to death from symptom onset ($\frac{1}{R_6} + \frac{1}{R_7} + \frac{1}{R_{10}}$ days) can be between 13.5 to 29 days. Therefore, 1 of them was placed randomly in between Feb 23 and Mar 8 to have a symptom onset, and the other was placed in between Mar 12 and Mar 27 to have a symptom onset. The 29 people who did not provided any

symptom onset information, had been distributed randomly to have a symptom onset at a random date over the whole period for which people in Ischgl reported an onset of a symptom, i.e., the period from 26th of January to 24th of April. These 31 people (29 + 2) had been assumed to also have loss of smell/loss of taste, and hence a similar random distribution of these 31 was done while working with the loss of smell/loss of taste data. When a non-specific time for symptom onset (for example, mid-March) was provided, corresponding cases were randomly distributed over 7 days around the non-specific time-point. For example, if N people answered mid-March, those N people were randomly distributed over a period of Mar 12 to Mar 18. In case a month in general was mentioned as a non-specific answer, persons with such answers were randomly distributed over the corresponding month to have a symptom onset. Based on the odds ratios for the period until 3rd week of February as compared to that of March, a significant overlap with the flu-season in Ischgl until 3rd week of February and officially accepted course of the outbreak in Ischgl, we have considered the symptomatic cases until Feb 22 to be non-specific for COVID-19. Symptoms until Feb 22 could not be clearly attributed to COVID-19 infections. Based on sero-positivity such cases were considered as asymptomatic in order to define the fraction of asymptomatic patients in the model. Following the data smoothing procedures mentioned above, there were 61 symptomatic cases before Feb 23rd, which were considered as asymptomatic. Hence, the analysis for any symptom onset consists of 490 – 61 = 429 individuals. In this case, α = (626 – 429)/626 = 0.3147. As 11 people among these went to hospital, ρ = 11/429 = 0.026 in this case. For analysis with onset data of anosmia/dysgeusia, we have considered individuals reporting any other symptom (OR much lower as compared to anosmia/dysgeusia) as asymptomatic seropositive. Furthermore, as cases before Feb 23 have been considered to be asymptomatic, after the corrections for 31 people mentioned above as well as for the people with non-specific onset date for anosmia/dysgeusia as per a similar procedure to that of the analysis based on any symptom onset, a number of 267 people were considered to have onset of anosmia/dysgeusia. Hence, in this case, α = (626 – 267)/626 = 0.5735. Now among these 267 people, 11 have gone to the hospital, which gives ρ = 11/267 = 0.0412. Among 11 people who went to hospital, 3 had needed ICUs including the two people who died, providing us with $\vartheta = \frac{3}{11}, \delta = \frac{2}{3}$. As we know the serostatus of all the 1473 people (size of the sub-population in our model) in our study and consider the symptom (or anosmia/dysgeusia) onset data for the serologically positive people, no symptomatic person among the seropositive individuals remain undetected ($\mu = 1$) in our computational analysis. To invoke a day/night symptom onset pattern, we assumed that there was a delay of 12 hours between actual onset of symptom(s) and the date the symptomatic individuals mentioned to have developed a symptom, resulting in $\tau = 2/day$.

Initial conditions:

As 2 dead people were considered in the study, the total initial population was 1475, among which the cases of the first day were exposed before $\frac{1}{R_2} + \frac{1}{R_3} + \frac{1}{\tau}$ days and the rest were susceptible. The cases reported on the second, third and fourth days were also considered as exposed before $\frac{1}{R_2} + \frac{1}{R_3} + \frac{1}{\tau}$ days.

General comment on determining R_0:

We fitted the parameters in Table MS1 to the data from 23rd of February to 16th of March 2020 and obtained the best parameter sets which minimize the cost functions for the data observed until March 16, to determine the basic reproduction number R_0. For details, see fitting strategy in the supplementary information.

Fitting strategy:

Step 1:

Strategy a. Fit the data (total symptomatic cases after data smoothening as explained above and total deaths) over a range of days until 16th of March 2020 to get an estimate of parameters using global optimization. The timespan till 16th of March was a period where NPIs were not likely to show an impact. First, we obtain best fit for the first 13 days (Feb 23 – Mar 6), 14 days (Feb 23 – Mar 7), 15 days (Feb 23 – Mar 8), 16 days (Feb 23 – Mar 9) and so on, until the first 23 days (Feb 23 – Mar 16). After completion of this step, we will have 11 best parameter sets for one trial corresponding to each of the above-mentioned stretches, all explaining these different durations of the phase before non-pharmacological interventions (NPIs) were likely to show an impact. We repeat this step 10 times to obtain 11 x 10 = 110 parameter sets. The *'interior-point'* method [8] was used in inbuilt *MATLAB* function *'fmincon'* as an optimization algorithm while carrying out *'GlobalSearch'* [9] with 3000 starting points in *MATLAB Release 2018a.* The starting points from which the optimization begins were then auto selected based on the parameter bounds and constraints. The logic of such a strategy comes from the fact that in a non-restricted scenario of the outbreak, if we capture the behaviour of the initial exponential phase well, we would be able to fit the whole exponential phase (before NPIs start to show an impact) with the resulting parameter sets obtained by fitting different stretches of this phase starting from day one.

Strategy b. Fit the data (total symptomatic cases after data smoothening as explained above and total deaths) from 23rd of February until 16th of March 2020 in a single stretch to get an estimate of parameters using global optimization. We repeat this for 110 trials. For each of these 110 trials, we not only save the minima providing the lowest cost function for fitting the data points from Feb 23 – Mar 16, but also save all other obtained minima. The *'interior-point'* method [8] was used in inbuilt *MATLAB* function *'fmincon'* as an optimization algorithm while carrying out *'GlobalSearch'* [9] with 3000 starting points in *MATLAB Release 2018a.* The starting points from which the optimization begins were then auto selected based on the parameter bounds and constraints. The logic of such a strategy comes from the fact that the timespan till 16th of March was a period where NPIs were not likely to show an impact.

Step 2:

Strategy a. For each of the 110 fitted parameter sets obtained from Step 1 - Strategy a, we now calculate the cost functions (normalized sum of squared residuals) which result from fitting the data points corresponding to Feb 23 – Mar 16 in a single stretch. This results in 110 cost function values each of which is associated with one particular fitted parameter set. Let us denote the minimum value of the cost function with Min_a, which gives us the best parameter set for Step 2 – Strategy a.

Strategy b. For each of the 110 fitted parameter sets obtained from Step 1 - Strategy a, we now calculate the cost functions (normalized sum of squared residuals) which result from fitting the data points corresponding to Feb 23 – Mar 6, Feb 23 – Mar 7, Feb 24 – Mar 8 and so on, until Feb 23 – Mar 16, thereby obtaining 11 cost functions values for each of them. Next, for each of these 110 parameter sets, we calculate the median value of these 11 cost functions obtained from the fitting of different stretches since Feb 23. This results in 110 median values each of which is associated with one particular fitted parameter set. Let us denote the minimum value of the median with Min_b, which gives us the best parameter set for Step 2 – Strategy b.

Strategy c. For each of the 110 fitted parameter sets obtained from Step 1 - Strategy a, we now calculate the cost functions (normalized sum of squared residuals) which result from fitting 10 unique data points randomly selected from the period of Feb 23 – Mar 16 for 1000 iterations. We then calculate the median of these 1000 cost functions for each of the 110 fitted parameter sets. This results in 110 median values each of which is associated with one particular fitted parameter set. Let us denote the minimum value of the median with Min_c, which gives us the best parameter set for Step 2 – Strategy c.

Strategy d. 110 trials corresponding to Step 1 - Strategy b resulted in 110 best fitted parameter sets, each corresponding to one trial. For each of these parameter sets, we now calculate the cost functions (normalized sum of squared residuals) which result from fitting the data points corresponding to Feb 23 – Mar 16 in a single stretch. This results in 110 cost function values each of which is associated with one particular fitted parameter set. Let us denote the minimum value of the cost function with Min_d, which gives us the best parameter set for Step 2 – Strategy d.

Strategy e. As mentioned in Step 1 – Strategy b, for each of the associated 110 trials, we also save all other minima obtained by the fitting algorithm along with the best ones. In this strategy, we collect all the minima (which also include the best ones) and obtain the corresponding cost functions (normalized sum of squared residuals) resulting from fitting the data points corresponding to Feb 23 – Mar 16 in a single stretch. This results in $110 \times L$ cost function values where each of them is associated with one particular fitted parameter set resulted in a minima and L is the total number of such minima obtained by all 110 trials. Let us denote the minimum value of the cost function with Min_e, which gives us the best parameter set for Step 2 – Strategy e. It is obvious to note that $Min_d = Min_e$.

Step 3: Step 2 - Strategy a resulted in better fit quality for the period of Feb 23 – Mar 16 for the parameter sets obtained from Step 1 – Strategy a. From Step 2 – Strategy a, we now choose the parameter sets that give us cost functions less than $1.125 \times Min_a$ for the period of Feb 23 – Mar 16 for subsequent analysis and generation of the figures (both in the main text and in the supplementary information). For each of these sets, we plot and verify whether they fit to the cumulative cases of symptom onset till Mar 16. Parameter sets selected based on other strategies are used for checking robustness (see Table MS2) of our reported values of R_o as obtained from Step 2 – Strategy a with the parameter sets that give us cost functions less than $1.125 \times Min_a$.

Step 4: Obtain R_0 with the equation above for each of these parameter sets.

Step 5: Use parameter sets obtained from Step 3 and estimate R_1 (contact frequency dependent transmission rate) in a shifting time-window using a global optimization method and multiple starting points (we use 42 starting points for each performed fitting in each window). For details of the implemented global optimization method, see Step 1.

Step 6: Calculate R_t (note, R_t can be more than R_0 due to temporal fluctuation) and report for each of the windows and for each of the best parameter sets.

Robustness Analysis:

Data	Strategy	Selection of Parameter Sets	Minimum R_0	Maximum R_0	Median R_0	Median Seroprevalence for Herd Immunity
Onset of any symptom since Feb 23, 2020	Step 2 - Strategy a	$< (1.125 \times Min_a)$	2.8	3.2	3.0	66.7%
		$< (1.250 \times Min_a)$	2.4	3.2	2.8	64.3%
		$< (1.375 \times Min_a)$	2.4	3.2	2.8	64.3%
	Step 2 - Strategy b	$< (1.125 \times Min_b)$	2.4	2.6	2.5	60.0%
		$< (1.250 \times Min_b)$	2.4	2.9	2.7	63.0%
		$< (1.375 \times Min_b)$	2.4	3.1	2.7	63.0%
	Step 2 - Strategy c	$< (1.125 \times Min_c)$	2.5	3.2	3.0	66.7%
		$< (1.250 \times Min_c)$	2.4	3.2	2.8	64.3%
		$< (1.375 \times Min_c)$	2.4	3.2	2.8	64.3%
	Step 2 - Strategy d	$< (1.125 \times Min_d)$	2.7	3.6	3.1	67.7%
		$< (1.250 \times Min_d)$	2.7	3.6	3.1	67.7%
		$< (1.375 \times Min_d)$	2.7	3.6	3.1	67.7%
	Step 2 - Strategy e	$< (1.125 \times Min_e)$	2.7	3.6	3.1	67.7%
		$< (1.250 \times Min_e)$	2.5	3.6	3.0	66.7%
		$< (1.375 \times Min_e)$	2.5	3.6	3.0	66.7%
Onset of anosmia/ Dysgeusia since Feb 23, 2020	Step 2 - Strategy a	$< (1.125 \times Min_a)$	3.1	3.7	3.3	69.7%
		$< (1.250 \times Min_a)$	3.0	3.7	3.3	69.7%
		$< (1.375 \times Min_a)$	2.9	3.7	3.2	68.8%
	Step 2 - Strategy b	$< (1.125 \times Min_b)$	2.9	3.4	3.2	68.8%
		$< (1.250 \times Min_b)$	2.9	3.7	3.2	68.8%
		$< (1.375 \times Min_b)$	2.9	3.7	3.2	68.8%
	Step 2 - Strategy c	$< (1.125 \times Min_c)$	3.1	3.7	3.3	69.7%
		$< (1.250 \times Min_c)$	3.0	3.7	3.3	69.7%
		$< (1.375 \times Min_c)$	2.9	3.7	3.2	68.8%
	Step 2 - Strategy d	$< (1.125 \times Min_d)$	3.1	3.7	3.4	70.6%
		$< (1.250 \times Min_d)$	3.1	3.7	3.4	70.6%
		$< (1.375 \times Min_d)$	3.1	3.7	3.4	70.6%
	Step 2 - Strategy e	$< (1.125 \times Min_e)$	3.0	3.9	3.5	71.4%
		$< (1.250 \times Min_e)$	3.0	3.9	3.5	71.4%
		$< (1.375 \times Min_e)$	3.0	3.9	3.5	71.4%

Table MS2. Robustness analysis. Estimated bounds of R_0 with its median value and seroprevalence corresponding to the median R_0 values for different case onset data and different methodology. See fitting strategy in the supplementary information for details of the strategies.

References:

[1] Mitra, Tanmay, et al. *Data based state-specific mathematical modelling, Rt estimation, and adaptive future prediction for COVID-19 outbreak and usage of healthcare system in India* (2020) http://india.secir.theoretical-biology.de

[2] Mitra, Tanmay, and Khailaie, Sahamoddin, et al. *Development of the reproduction number from coronavirus SARS-CoV-2 case data in Germany and implications for political measures.* medRxiv (2020) doi: https://doi.org/10.1101/2020.04.04.20053637

[3] Lauer, Stephen A., et al. *The Incubation Period of Coronavirus Disease 2019 (COVID-19) From Publicly Reported Confirmed Cases: Estimation and Application.* Annals of Internal Medicine 172.9 (2020): 577-582.

[4] Nishiura, Hiroshi, Natalie M. Linton, and Andrei R. Akhmetzhanov. *Serial interval of novel coronavirus (COVID-19) infections.* International journal of infectious diseases (2020).

[5] Diekmann, Odo, Johan Andre Peter Heesterbeek, and Johan AJ Metz. *On the definition and the computation of the basic reproduction ratio R0 in models for infectious diseases in heterogeneous populations.* Journal of mathematical biology 28.4 (1990) 365-382.

[6] Van den Driessche, Pauline, and James Watmough. *Reproduction numbers and sub-threshold endemic equilibria for compartmental models of disease transmission.* Mathematical biosciences 180.1-2 (2002) 29-48.

[7] Van den Driessche, P., and James Watmough. *Further notes on the basic reproduction number.* Mathematical epidemiology (2008). 159-178.

[8] Byrd, R.H., Mary E. Hribar, and Jorge Nocedal. *An Interior Point Algorithm for Large-Scale Nonlinear Programming.* SIAM Journal on Optimization, Vol 9, No. 4, pp. 877–900, 1999.

[9] Ugray, Zsolt, Leon Lasdon, John Plummer, Fred Glover, James Kelly, and Rafael Martí. *Scatter Search and Local NLP Solvers: A Multistart Framework for Global Optimization*. INFORMS Journal on Computing, Vol. 19, No. 3, 2007, pp. 328–340.